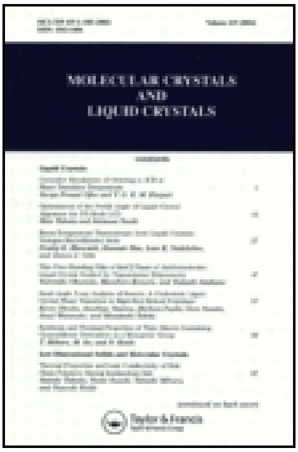

Molecular Crystals and Liquid Crystals
Publication details, including instructions for authors and subscription information:
http://www.tandfonline.com/loi/gmcl20

Temperature Dependence of the Bistable Photoconductivity of Thin DNA: PEDOT Films

V. Kažukauskas [a], M. Pranaitis [a], A. Sakavičius [a], O. Krupka [b], F. Kajzar [b c] & B. Sahraoui [c]

[a] Semiconductor Physics Department and Institute of Applied Research, Vilnius University, Saulėtekio al. 9, bldg. 3, LT-10222, Vilnius, Lithuania

[b] POLITEHNICA University of Bucharest, Faculty of Applied Chemistry and Materials Science, Str. Polizu nr. 1, Bucharest, Romania

[c] MOLTECH Anjou - UMR CNRS 6200 MINOS, University of Angers, 2 Boulevard Lavoisier, 49045, Angers, France

To cite this article: V. Kažukauskas, M. Pranaitis, A. Sakavičius, O. Krupka, F. Kajzar & B. Sahraoui (2012): Temperature Dependence of the Bistable Photoconductivity of Thin DNA: PEDOT Films, Molecular Crystals and Liquid Crystals, 554:1, 83-94

To link to this article: http://dx.doi.org/10.1080/15421406.2012.633798

Mol. Cryst. Liq. Cryst., Vol. 554: pp. 83–94, 2012

ISSN: 1542-1406 print/1563-5287 online
DOI: 10.1080/15421406.2012.633798

Temperature Dependence of the Bistable Photoconductivity of Thin DNA: PEDOT Films

V. KAŽUKAUSKAS,[1,*] M. PRANAITIS,[1] A. SAKAVIČIUS,[1]
O. KRUPKA,[2] F. KAJZAR,[2,3] AND B. SAHRAOUI[3]

[1]Semiconductor Physics Department and Institute of Applied Research,
Vilnius University, Saulėtekio al. 9, bldg. 3, LT-10222 Vilnius, Lithuania
[2]POLITEHNICA University of Bucharest, Faculty of Applied Chemistry
and Materials Science, Str. Polizu nr. 1, Bucharest, Romania
[3]MOLTECH Anjou - UMR CNRS 6200 MINOS, University of Angers,
2 Boulevard Lavoisier, 49045 Angers, France

Thin DNA:PEDT-PSS layers were investigated. The functionalization of DNA by PEDT-PSS rendered the material electrically active, its conductivity being about (1–5) $\times$ *10^{-10} Ω^{-1}cm^{-1} at the room temperature. The samples remained ohmic down to 77 K. The thermal activation energy of the conductivity near the room temperature was about 0.033 eV, and it decreased under 0.014 eV below 170–180 K. The weak carrier trapping was identified by the Thermally Stimulated Current method, proving the recombination of light-generated carriers. Notably, by constant light excitation a "bistable" photoconduction below the room temperature was evidenced. The photosensitive state could be induced by the light from the spectral region from* $\sim$ *500 nm up to* $\sim$*1000 nm, with a maximum effect in the range of 650–800 nm. A remarkable increase of the photocurrent could be observed below 145–155 K by cooling the samples. Meanwhile by heating the photosensitivity remained increased up to 235–245 K. The long characteristic relaxation times after the light excitation in this state were proportional to the relative photosensitivity of material. This indicates that such phenomenon could presumably be attributed to the light-induced changes associated with PEDT-PSS, i.e., modification of the sample material morphology and/or induced variation of carrier transport conditions.*

Keywords Carrier trapping; deoxyribonucleic acid (DNA); electrical conductivity; light absorption ; PEDOT; photoconductivity

PACS 87.14.gk; 81.40.Tv; 81.40.Rs; 73.50.Gr.

1. Introduction

Nucleic acids and their derivatives attract a lot of attention of researchers because of their important biological role [1,2]. At the same time deoxyribonucleic acid (DNA), which exhibits a charge migration, is a subject of interest for its physical properties, and particularly for a great potential of application in photonics and in molecular electronics. Such applications include devices based on second and third order nonlinear optical (NLO)

---

[*] Address correspondence to V. Kažukauskas, Department of Semiconductor Physics and Institute of Applied Research, Vilnius University, Saulėtekio 9, bldg.3, LT-10222 Vilnius, Lithuania. Tel.: (+370-5) 2366 035; Fax: (+ 370-5) 2366 003; E-mail: vaidotas.kazukauskas@ff.vu.lt

effects [3], low loss optical waveguides [4], holography [5,6], organic photovoltaics and organic field effect transistors (FET) [7]. The nucleic base of DNA is 0.34 nm long with a diameter of the helix about 2 nm. Therefore, the double helix with a π–π^* stacking structure of nucleobase pairs of DNA forms a tunnel suitable for electron transfer. The relatively weak π–π^* electron conjugation renders materials with a large optical transparency window. Duplex structures in the fibres have been studied by X-ray diffraction and solid state by NMR [8–10].

However, pure DNA is electrically passive material. In order to render it active one has to functionalize it with poly(3,4-ethylenedioxythiophene) (PEDOT, PEDT) and poly(styrenesulfonate) (PSS) complex. PEDT-PSS is a promising polymer for electronic applications because it is solution processable. When dried, PEDT-PSS coatings have low resistivity, excellent water resistance, and high transmittance of visible light. PEDT-PSS can be included in the DNA matrix by intercalation in stacked layers of nucleic acid bases of the helix, by inserting into the major and minor grooves of DNA helix or by electrostatically stacking on the surface of DNA helix [11–13]. This enables engineering of the electrical properties of the material. Nevertheless, to assure the controllable purposeful modification of these properties, extensive investigations are still required. In this paper we report investigations of photo-electrical properties of DNA:PEDT-PSS thin films. The films were characterized by the UV and visible spectroscopy. Their electrical and photo-conductivity depending on the temperature and excitation by light was analysed.

2. Samples and Experiment

Poly(3,4-ethylenedioxythiophene) and poly(styrenesulfonate) (Fig. 1) aqueous dispersion of the intrinsically conductive polymer PEDT-PSS has been commercialised as the trade mark of BAYTRON® PH 500 being especially homogenized to achieve small size particles. The weight ratio of PEDT to PSS is about 1:2.5. This waterborne dispersion is ready to use and can be deposited by spincoating with viscosity max. 30 mPa·s [14]. It is tailored to a high conductivity and forms conductive coatings. This kind of polymer is transparent, its coatings are colourless to bluish, and they have good resistance to hydrolysis, good photo

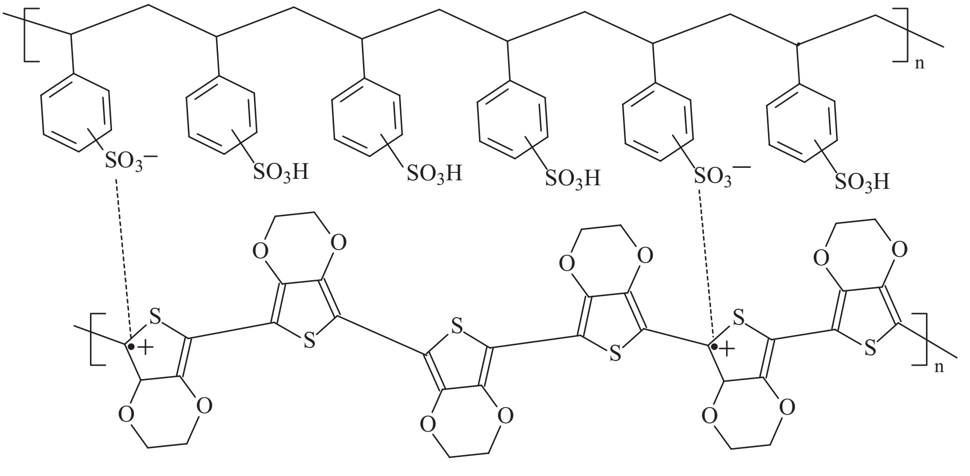

Figure 1. Chemical structure of polymer complex PEDOT (PEDT-PSS).

stability and good thermal stability. Their absorption is high in the range of 900 to 2000 nm, and weak in the visible spectrum up to 800 nm [15].

DNA sodium salts, extracted from salmon milt and roe, were provided by CIST. They were separated from other constituents. The procedure of obtaining pure DNA includes homogenization, enzyme treatment, protein elimination by controlling the pH level to 7.5, carbon treatment and precipitation by adding acetone. The purified DNA was finally filtered from the acetone and freeze dried [16]. The purified DNA dissolves only in water. It does not dissolve in any organic solvent, except a strong acidic solvent such as trifluoromethansulfonic acid [4]. The molecular weight measured $M_W = 10^6$ Daltons (Da) or 2000 base pairs. The high molecular weight DNA rendered inhomogeneous film thickness due to high solution viscosity. In order to reduce the viscosity of the DNA-based solutions it was necessary to reduce the mean MW using sonication by ultrasonic procedure to 200 kDa 300 bp and a chain length of 0.1 μm for improved film uniformity and increased poling efficiency [17]. After sonication of DNA (8 g/L) in 18 MΩ cm deionized water, at 20°C, it was blended using a magnetic stirrer overnight and then DNA solution was added to PEDT-PSS aqueous solution with different volume ratios 1:0.2 and 1:0.5 of DNA:PEDT-PSS.

The solutions of polymers were spin-coated at 500 or 1200 rpm on the ITO glass substrates which were cleaned in various solvents. Immediately after the deposition, the thin films were cured in an 50°C oven in order to eliminate any remaining solvent. The thickness of the thin solid films was measured by profilometer *Tencor, ALFA-Step* and was found 0.3–1.5 μm. The semi-transparent aluminium contacts were evaporated on the top. Alternatively some samples were deposited on the gridded intercalated electrodes initially evaporated on glass substrates.

The films were characterized by the UV and visible spectroscopy. Their Current-Voltage (IV) and conductivity temperature dependencies were measured by Keithley electrometer-voltage source Model 6430 from 77 K up to 300 K depending on the light excitation. The white light from the 100 W halogen lamp was used to investigate photoconductivity. To analyse photosensitivity of the material depending on the spectral range of the exciting light the long- and short-pass colour filters with different cut-off wavelengths ranging from 400 nm up to 1000 nm were used.

3. Results and Discussion

3.1. Light Absorption Spectra

The UV-VIS-NIR absorption spectra of studied molecules in thin films deposited on glass substrates were measured at room temperature with a PERKIN ELMER UV/VIS/NIR Lambda 19 spectrometer. In Fig. 2 absorption spectrum of a DNA:PEDT-PSS (1:0.5) thin film on the BK7 glass substrates is presented. A strong UV absorption absorption band from 250 to 300 nm is seen [18]. It corresponds to the π-π^* transition of electrons of the C=C bond of the DNA bases. Another wide and low absorption band at around 900 nm is associated with the conductive polymer PEDT-PSS [11].

3.2. Electrical Conductivity in the Dark

Sample conductivity at room temperature was in average about (1–5) × 10^{-10} Ω^{-1}cm^{-1}, though it could deviate by up to two orders of magnitude even in the samples produced on the same substrate, indicating sensitivity of their properties to the technological conditions. IV curves were linear and symmetrical down to 78 K temperature as it is shown in Fig. 3.

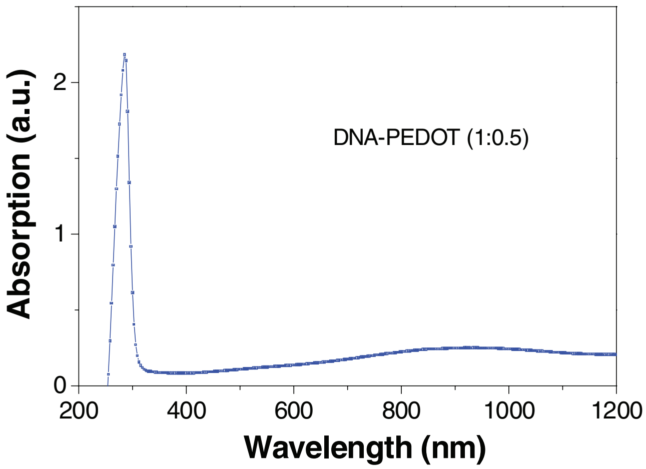

Figure 2. Absorption spectrum of a DNA-PEDOT (1:0.5) thin film.

To investigate carrier transport and thermal generation processes depending on temperature, temperature scans of the current were measured. In Fig. 4 the dark current and photocurrent temperature dependencies are presented. It can be seen that close to the room temperature their thermal activation energy is about 0.033–0.035 eV. These values were not dependent on the applied bias. Usually thermal activation energy values of DNA varying from 0.18 up to 1.4 eV are reported, depending on material and experimental conditions [19]. Such values are significantly higher than obtained here. This implies that in our samples influence of PEDOT is pronounced, as the conductivity of it is usually high and activation energy close to the room temperature is in meV range [20–22]. Similar reduction of activation energy down to 0.05 eV was observed in DNA-gold composite in [23].

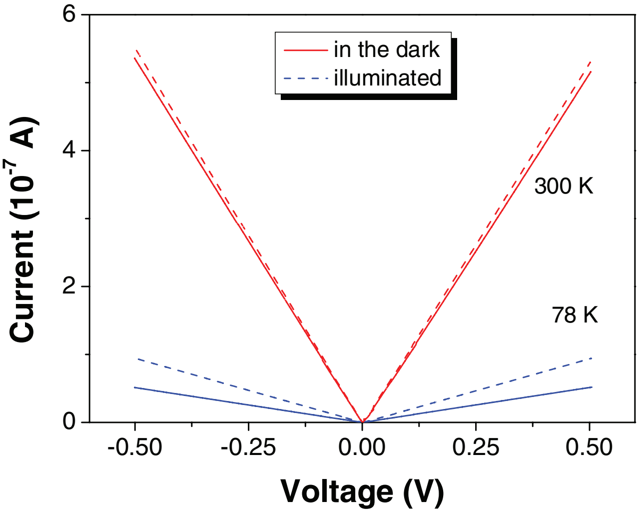

Figure 3. IV curves of the sample upon illumination by the white light (dashed curves) and in the dark (solid lines) at 300 K and 78 K as indicated on the Figure.

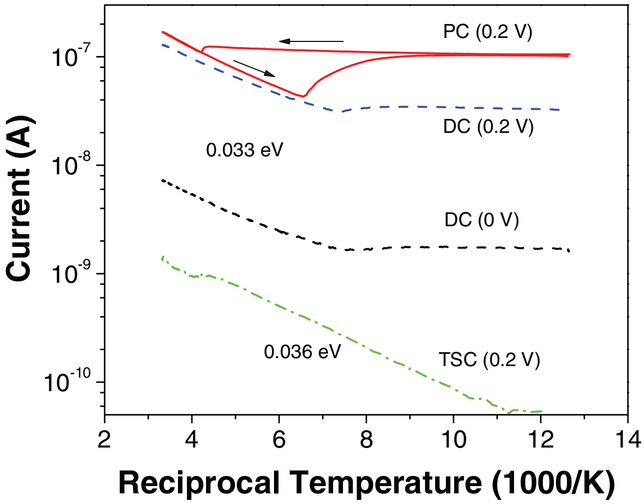

Figure 4. Temperature dependencies of the photocurrent (PC – solid curves), upon scanning the temperature down and up as indicated by the arrows, the dark current (DC – dashed curves) at 0.2 V bias and without any applied bias and the thermally stimulated current (TSC – dotted line).

Below about 130 K–140 K a characteristic kink appears, and the thermal activation energy drops below 0.014 eV, approaching in some samples zero values. Qualitatively similar trend was observed in DNA-gold composite in [23] because of the change of the charge transport mechanism. At higher temperatures the small polaron hopping model [24–26] was shown to be applicable to analyze the experimental data. This theory accounts for phonon assistance to electron hopping, and the electrical conductivity is given by:

$$\sigma = \sigma_0 \exp\left(-\frac{E_a}{kT}\right), \tag{1}$$

with

$$E_a(T) = kT \sum_q C_q \tanh\left(\frac{\hbar\omega_q}{4kT}\right), \tag{2}$$

where C_q and ω_q are the coefficient and molecular vibrational frequency, respectively. In contrast, in the low-temperature region electrical conductance was shown to proceed according to the Mott variable-range hopping model [26, 27]:

$$\sigma = \sigma_0 \exp\left(-\left(\frac{T_0}{T}\right)^{0.25}\right). \tag{3}$$

3.3. Carrier Trapping

To analyse the possible effect of carrier trapping in the observed phenomena, the Thermally Stimulated Currents (TSC) were investigated. The details of the TSC method are presented in [28–30]. This method was proven to be a sensitive tool enabling to reveal, e.g., differences caused by polar molecular orientation in organic films [31]. The TSCs are shown in

Fig. 4. Characteristically, TSCs are low as compared with both dark current and current after the light excitation. This indicates that relatively small number of carriers becomes trapped, and most of them recombine after the light excitation is turned off. Therefore presumably carrier trapping cannot be effectively involved in the observed conductivity behaviour. Moreover, nearly the same activation energy values as of the dark currents of about 0.036–0.043 eV were evaluated in a wider temperature region extending down to the lowest temperatures. This indicates that carrier trapping conditions remain unchanged in the whole temperature region, meanwhile properties of the photoconductivity change notably, as it will be discussed below. On the other hand such low activation energy values could be indication that current increase with temperature is related to transport phenomena, rather than change of the carrier density because of their thermal generation., i.e., growth of carrier mobility. Similar conclusion was made also for disordered P3HT-PCBM bulk-heterojunction organic Solar cell structures [32]. This assumption is realistic by having in mind complicated hopping transport character in disordered organic materials. Therefore evaluated activation energies could probably reflect the energetic spread in the charge transporting levels, resulting in distribution of the density of transporting states (DOS). Nevertheless to confirm this possibility by direct mobility measurements either by Time-Of-Flight (TOF) method, Charge Extraction by Linearly Increasing Voltage (CELIV) method or by other methods used for low mobility materials, special sample preparation and experimental arrangements are necessary, and this is our future task.

3.4. DC Photoconductivity

The samples had demonstrated photosensitivity starting from the room temperature down to 78 K as it is demonstrated in Fig. 3. At the room temperature the photocurrent used to grow up to ∼2–3 per cent upon the white light excitation, and at LN temperature its growth by a factor of up to two was observed. Dependence of the photocurrent on the temperature was quite complex. As it was mentioned above a characteristic kink was observed in the dark current measurements. Upon the light excitation it became even more expressed. A typical behaviour is presented in Fig. 4. It can be seen that by lowering the temperature the photocurrent starts growing at about 145–155 K and reaches saturation level that is by a factor of about (2–2.5) higher than that of the minimum. Afterwards, if the temperature is increased the photocurrent changes relatively little up to about 235–245 K, forming a "bistable" loop. This behaviour does not change with applied bias, indicating that the effect is light-induced. This is supported by the fact that sample reaction on the applied voltage and light pulses was different: upon application of a voltage step very fast increase of the current was observed, meanwhile the photocurrent growth was relatively slow and could be approximated well by the exponential dependence as it is indicated on Fig. 5 by the solid line. This evidences that different carrier transport mechanisms play a role in both cases. Upon application of the voltage pulse fast carrier injection from contacts takes place that is limited by ohmic conduction of the sample volume. Meanwhile slower light-induced generation of carriers occurs from their transport and/or trapping states. Current decay after the light is switched off occurs similarly, just with significantly longer relaxation time constants. To analyse the effect of the exciting light spectra we had measured the photoconductivity of the samples using the long- and short-pass colour filters, as shown in Fig. 6. The relative photoconductivity was calculated as: $\frac{I_{light}-I_{dark}}{I_{dark}}$. It can be seen that the relative photoconductivity increases upon excitation by light with the wavelengths ranging from ∼500 nm up to ∼ 1000 nm. The maximum is reached in the region from about

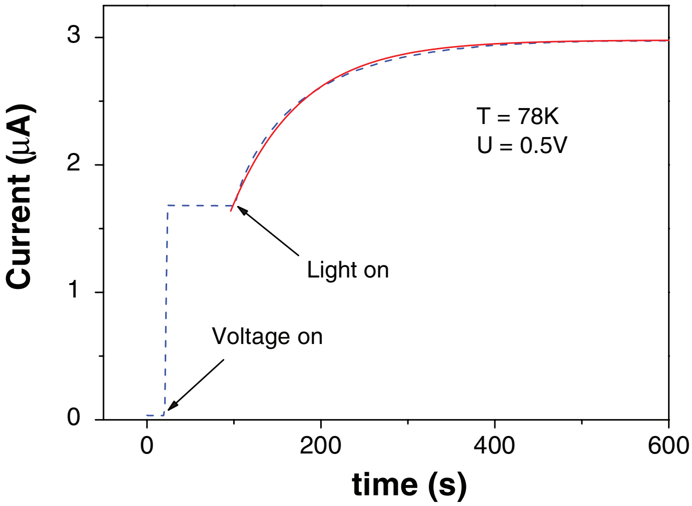

Figure 5. Sample reaction on applied voltage pulse and white light pulse (dashed curve) as indicated on the Figure. The photocurrent growth could be approximated well by exponential dependence as indicated by the solid curve.

~650 nm up to ~800 nm. This implies that this phenomenon could be associated with excitation of PEDT-PSS, demonstrating the absorption peak in the similar region (Fig. 2).

3.5. Transient Behaviour of the Photoconductivity

The transient behaviour of the photocurrent by scanning the temperature up and down upon illumination of the samples with the light pulse is presented in Fig. 7. The temperature

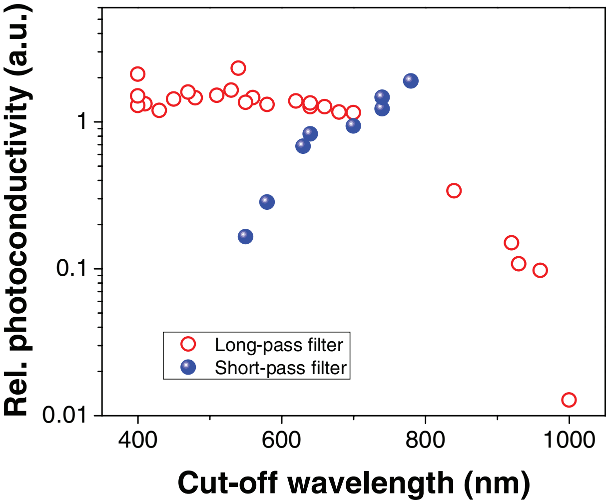

Figure 6. Relative photoconductivity values upon excitation of the sample through the short- and long-pass colour filters. The points on the Figure mark cut-off wavelengths of the filters.

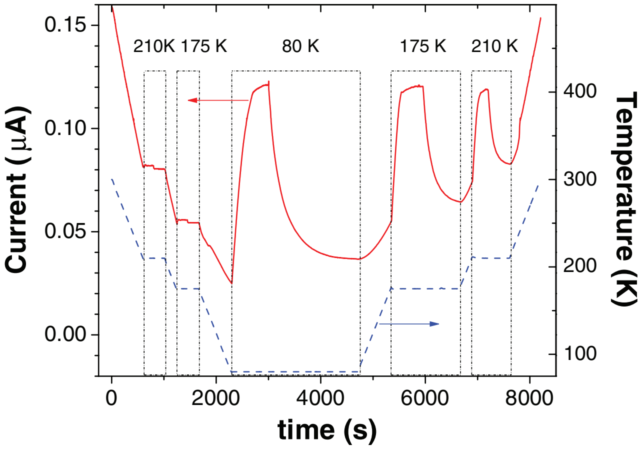

Figure 7. Change of the current upon variation of the temperature and illumination of the sample by light pulses at the stabilized temperatures. The temperature was stabilized at 210 K, 175 K, i.e., within the bistable loop, and at 80 K. Regions of the temperature stabilization are indicated by the dashed-dotted rectangles. The temperature values are indicated nearby. At these points the sample was excited by the white light which later on was switched off and the temperature scan was re-started.

was stabilized at 210 K, 175 K, i.e., within the bistable loop, and at 80 K. At these points the sample was excited by the white light which later on was switched off and the temperature scan was re-started. In Fig. 8 behaviour of the relative photoconductivity is presented. It can be seen that upon cooling the sample down to the characteristic kink point, the photosensitivity remains low, indicating that the heating of the sample by the light can be excluded. At the temperatures below this point the photocurrent increases

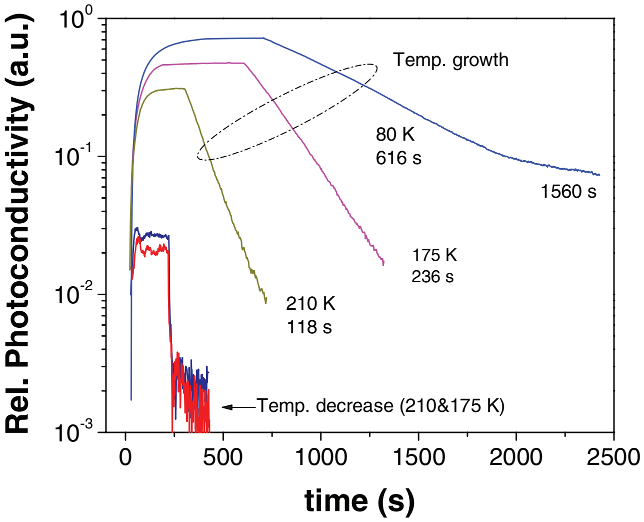

Figure 8. Kinetics of the relative photoconductivity upon excitation of the sample by the light pulse at different temperatures by cooling and heating.

significantly, moreover, its maximum reaches the same value upon heating the sample (Fig. 7). Meanwhile the relative photoconductivity reaches about 0.7 at 80 K (Fig. 8). It can be seen that the photocurrent upon illumination increases much faster than it drops after the light is turned off, though both processes could be approximated well by the single exponents with different time constants. This indicates appearance of the quite complex effect that cannot be attributed to the simple model, e.g., carrier generation from single trapping centres [33]. At 80 K relaxation time constant reached up to several hundreds of seconds, moreover even longer relaxation "tail" appears that could probably indicate appearance of the persistent photoconductivity phenomenon [34]. This phenomenon is associated with the conditions, at which light-generated carriers are unable to recombine, e.g., become trapped in the spatially separated potential wells and hills of the band gap edges in the disordered structure, slowing in this way the recombination. Upon heating the sample relaxation times used to shorten as indicated in Fig. 9. As seen from Fig. 9a) this shortening of the relaxation time constants is non-exponential due to the change of the transport and/or sample properties at the transition temperature. Characteristically, amplitudes of the relative photoconductivity had followed qualitatively similar behaviour, as it is demonstrated in Fig. 9b). This can be explained by the fact that the recombination of the light generated carriers is slowed down at lower temperatures, causing growth of the relative photoconductivity.

Therefore one can assume that the bistability effect of photoconductivity could probably be attributed to the light-induced morphology changes of the samples, resulting in a sudden increase of photosensitivity of material at low temperatures. To explain this effect several mechanisms can be accounted for. First of all, it is known that an anisotropic conductivity is characteristic for PEDT-PSS thin films [21]. So, one can suppose that light excitation could energize molecular movements of PEDT-PSS, changing in this way the predominant orientation of PSS lamellas. The light induced variation of PEDOT conjugation lengths was reported in [35]. Another possible mechanism could be variation of the transition temperature at which change of the transport mechanism occurs as described above. This could be assisted by the light-induced changing of the density of hopping states, because of their filling by generated carriers. Nevertheless to precise this effect the more detailed investigations are necessary and this is our future task.

Summary and Conclusions

We report investigations of DNA:PEDT-PSS thin films. After sonication of DNA in deionised water, DNA solution was added to PEDT-PSS aqueous solution with different ratios 1:0.2 and 1:0.5 of DNA:PEDT-PSS.

The solutions of polymers were spin-coated on the ITO glass substrates. The thickness of the obtained films was 0.3–1.5 μm. The semi-transparent aluminium contacts were evaporated on the top. The films were characterized by the UV and visible spectroscopy. Their conductivity temperature dependencies were measured from 77 K up to 300 K depending on the light excitation.

Sample conductivity at room temperature was in average about (1–5) × 10^{-10} Ω^{-1}cm^{-1}, though it could deviate by up to two orders of magnitude even in the samples produced on the same glass substrate indicating sensitivity of their properties to the technological conditions. IV curves were linear and symmetrical down to LN temperature. The thermal activation energy of the dark conduction near the room temperature was about 0.033 eV and it did not depend on the applied bias. We have identified weakly expressed

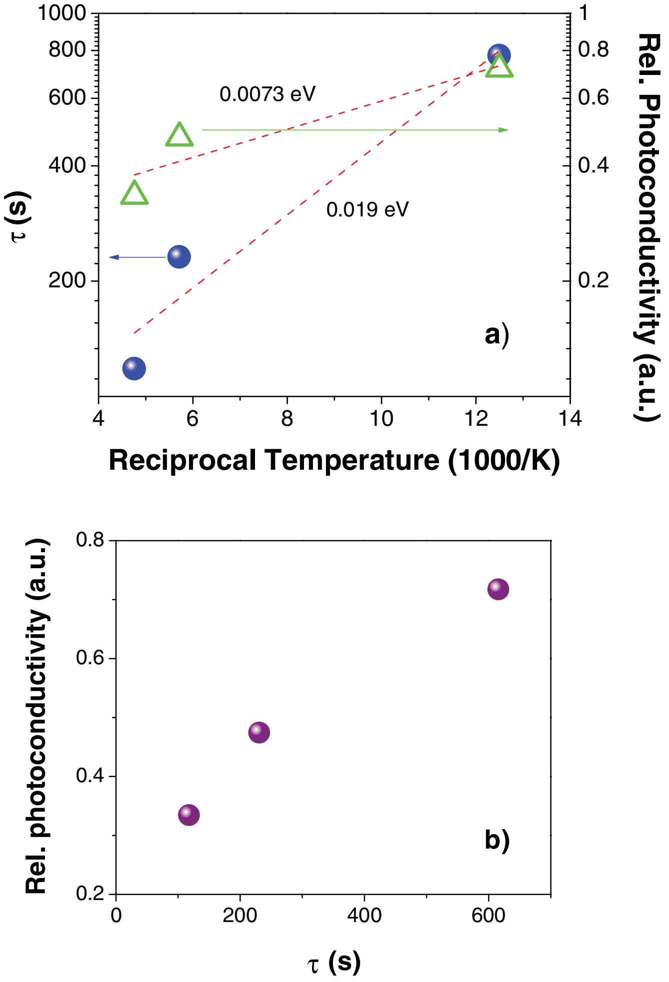

Figure 9. Temperature dependencies of the time constants of the exponents describing decay of the current after the white light pulse and the amplitude of the relative photoconductivity (a) and proportionality of the decay time constants and the relative photoconductivity (b).

carrier trapping by the Thermally Stimulated Current method, what proves the fast recombination and/or retrapping of light-generated carriers.

We had observed the photosensitivity of the samples that was dependent on the temperature. By constant light excitation a "bistable" photoconduction below the room temperature was evidenced. Only very small photoconductivity was observed by cooling the samples down to 145–155 K. Below this temperature sudden increase of the relative photoconductivity took place that reached up ~0.7 at 80 K. Meanwhile by heating the photosensitivity remained increased up to 235–245 K. The photosensitive state could be induced by the light from the spectral region from ~500 nm up to ~1000 nm, with a maximum effect in the range 650–800 nm. Characteristically, slow relaxations of the current after the light excitation took place, the time constant of which reached several hundreds of seconds at low temperature. The characteristic relaxation times after the light excitation in this state were proportional to the relative photosensitivity of material. The observed phenomena could presumably be attributed to the light-induced changes of the sample material morphology and/or associated variation of carrier transport conditions.

Acknowledgements

A. Sakavičius acknowledges Student Research Fellowship Award from the Lithuanian Science Council. F. Kajzar acknowledges the support of EU through the POS CEE ID_634/12575 project

References

[1] Dou, X., Takama, T., Yamaguchi, Y., Hirai, K., Yamamoto, H., Doi, S., & Ozaki, Y. (1998). *Appl. Opt.*, *37*, 759.

[2] Asayama, S., Maruyama, A., Cho, Ch.-S., & Akaike, T. (1997). *Bioconjugate Chem.*, *8*, 833.

[3] Krupka, O., El-Ghayoury, A., Rau, I., Sahraoui, B., Grote, J. G., & Kajzar, F. (2008). *Thin Solid Films*, *516*, 8932.

[4] Grote, J. G., Hagen, J. A., Zetts, J. S., Nelson, R. L., Diggs, D. E., Stone, M. O., Yaney, P. P., Heckman, E., Zhang, C., Steier, W. H., Jen, A. K.-Y., Dalton, L. R., Ogata, N., Curley, M. J., Clarson, S. J., & Hopkins, F. K. (2004). *J. Phys. Chem. B*, *108*, 8584.

[5] Fink, H.-W., Schmid, H., Ermantraut, E., & Schulz, T. (1997). *J. Opt. Soc. Am. A*, *14*, 2168.

[6] Czaplicki, R., Krupka, O., Essaidi, Z., El-Ghayoury, A., Kajzar, F., Grote, J. G., & Sahraoui, B. (2007). *Opt. Express*, *15*, 15269.

[7] Singh, B., Sariciftci, N. S., Grote, J. G., & Hopkins, F. K. (2006). *J. Appl. Phys.*, *100*, 024514.

[8] Tanaka K., & Okahata, Y. (1996). *J. Am. Chem. Soc.*, *118*, 10679.

[9] Leslie, A. G. W., Arnott, S., Chandrasekaran, R., & Ratliff, R. L. (1980). *J. Mol. Biol.*, *143*, 49.

[10] Alam, T. M., Orban, J. & Drobny, G. (1990). *Biochemistry*, *29*, 9610.

[11] Wagenknecht, H. (2002). *Chem. Unserer Zeit*, *36*, 318.

[12] Tang, L., Sun, Z., Guo, J., & Wang, Z. (2006). *Chin. Opt. Lett.*, *4*, 101.

[13] Zhang, G., Takahashi, H., Wang, L., Yoshida, J., Kobayashi, S., Horinouchi, S., & Ogata, N. (2002). *Proc. SPIE*, *4905*, 375.

[14] Product information *CLEVIOS*™ PH 500, http://www.clevios.com.

[15] Kymakis, E., Klapsis, G., Koudoumas, E., Stratakis, E., Kornilios, N., Vidakis, N., & Franghiadakis, Y. (2007). *Eur. Phys. J. Appl. Phys.*, *36*, 257.

[16] Grote, J., Diggs, D., Nelson, R., Zetts, J., Hopkins, F., Ogata, N., Hagen, J., Heckman, E., Yaney, P., Stone, M., & Dalton, L. (2005). *Mol. Cryst. Liq. Cryst.*, *426*, 16.

[17] Heckman, E., Hagen, J., Yaney, P., Grote, J., & Hopkins, F. (2005). *J. Appl. Phys. Lett.*, *87*, 211115.

[18] Wang, L., Yoshida, J., Ogata, N., Sasaki, S., & Kajiyama, T. (2001). *Chem. Mater.*, *13*, 1273.

[19] Bellido, E. P., Bobadilla, A. D., Rangel, N. L., Zhong, H., Norton, M. L., Sinitskii, A., & Seminario, J. M. (2009). *Nanotechnology*, *20*, 175102.

[20] Kim, J. Y., Jung, J. H., Lee, D. E., & Joo, (2002). *J. Synthetic Metals*, *126*, 311.

[21] Nardes, A. M., Kemerink, M., Janssen, R. A. J., Bastiaansen, J. A. M., Kiggen, N. M. M., Langeveld, B. M. W., van Breemen, A. J. J. M., & de Kok, M. M. (2007). *Adv. Mater.*, *19*, 1196.

[22] Sangeeth, C. S. S., Jaiswal, M., & Menon, R. (2009). *J. Phys.: Condens. Matter*, *21*, 072101.

[23] Kodama, T., Jain, A., & Goodson, K. E. (2009). *Nanoletters*, *9*, 2005.

[24] Tran, P., Alavi, B., & Gruner, G. (2000). *Phys. Rev. Lett.*, *85*, 1564.

[25] Inomata, A., Shimomura, T., Heike, S., Fujimori, M., Hashizume, T., & Ito, K. (2006). *J. Phys. Soc. J.*, *75*, 074803.

[26] Boettger, H., & Bryksin, V. V. (1985). Hopping conduction in Solids, Akademie-Verlag: Deerfield Beach, FL, USA.

[27] Kaynak, A. (1985). *Tr. J. Chem.*, *22*, 81.

[28] Simmons, J. G., & Taylor, G. W. (1977). *Phys. Rev. B*, *5*, 1619.

[29] Kavaliauskienė, G., Kažukauskas, V., Rinkevičius, V., Storasta, J., Vaitkus, J. V., Bates, R., O'Shea, V., & Smith, K. M. (1999). *Appl. Phys. A*, *69*, 415.

[30] Kažukauskas, V. (2004). *Semicond. Sci. Technol.*, *19*, 1373.

[31] Kažukauskas, V., Čyras, V., Pranaitis, M., Apostoluk, A., Rocha, L., Sicot, L., Raimond, P., & Sentein, C. (2007). *Org. Electron.*, *8*, 21.

[32] Kažukauskas, V., Arlauskas, A., Pranaitis, M., Glatthaar, M., & Hinsch, A. (2010). *J. Nanosci. Nanotechnol.*, *10*, 1376.

[33] Seeger, K. (2002). Semiconductor Physics. An Introduction. Ch. 12, *Photoconductivity*, 8th Ed. Berlin, Germany: Springer: p. 402–416.

[34] Sheinkman, M. K., & Shik, A. Y. (1976). *Sov. Phys. Semicond.*, *10*, 128.

[35] Marciniak, S., Crispin, X., Uvdal, K., Trzcinski, M., Birgerson, J., Groenendaal, L., Louwet, F., & Salaneck, W. R. (2004). *Synthetic Metals*, *141*, 67.